Electronic Supplementary Material (ESI) for Lab on a Chip.

Supplementary Information

Stability Analysis of Chemically Modified mRNA Using Micropattern-Based Single-Cell Arrays

M. Ferizi[1], C. Leonhardt[2], C. Meggle[2], M.K. Aneja[3], C. Rudolph[3], C. Plank[1,3] and J. O. Rädler[2,*]

[1] Institute of Experimental Oncology and Therapy Research, Technical University of Munich, Munich, 81675 Germany

[2] Faculty of Physics and Center for NanoScience, Ludwig Maximilian University, Munich, 80539 Germany

[3] Ethris GmbH, Martinsried, 82152 Germany

* To whom correspondence should be addressed. Tel: +49 89 2180 2438; Fax: +49 89 2180 3182; Email: raedler@lmu.de

The authors wish it to be known that, in their opinion, the first two authors should be regarded as Joint First Authors.

Table S1: Secondary structures (mfold)

d2EGFP	∆ G	5'end	3' end	5' UTR	3'UTR
control	-358,9	partial binding with cds (8/8)	loose (8/8)	none	none
5' CYBA	-375	partial binding with 5' CYBA UTR (7/8)	loose (8/8)	binds with cds (6/8)	none
3' CYBA	-411,6	partial binding with 3' CYBA UTR (8/8)	binds with 5'end (4/4)	none	forms one hairpin (7/8)
5'+3' CYBA	-405,7	binds with 3' CYBA UTR (3/8)	binds with 5'end (4/4)	binds with 3' CYBA UTR (4/8)	forms one hairpin (7/8)
5'+2x3' CYBA	-437,7	binds with 3'UTR (8/8)	loose (8/8)	binds with 3'UTR and gene (6/8)	1st 3'UTR: hairpin; 2nd 3'UTR: hairpin (7/8)
2x3' CYBA	-444,1	binds with itself and forms hairpin (8/8)	loose (7/8)	none	1st 3'UTR: hairpin; 2nd 3'UTR: two hairpins (3/8)

In Table S1, features of the mRNA constructs such as free minimum energy (∆G) and secondary structures found at both ends and within the UTRs are listed. The folding platform mfold was used to predict mRNA secondary structures (1). For each construct, we compared the eight secondary structures that have the highest free energy. The highest free energy values are predicted for the 2x3' UTR and the 3' UTR constructs. The 5' end of each mRNA

construct partially binds with the 3'UTR or the 5'UTR, except for the control construct, which binds to the coding sequence (cds). Interestingly, the 5' end of the 2x3' mRNA construct forms a stabilizing hairpin with itself. However, hairpin loops near the 5' end can also hinder protein translation (2). Another feature was found in the 3' end of the 3' UTR and 5'+3' UTR mRNA constructs: There, the 3' end binds with the 5' end, minimizing the distance from each other and thus can enable faster initiation of translation. Unlike the 5'UTRs, the 3' UTR of each mRNA construct forms at least one hairpin with itself.

Table S2: Human CYBA and its UTRs

Untranslated region	**DNA sequence (from 5' to 3')**
5'	CGCGCCTAGCAGTGTCCCAGCCGGGTTCGTGTCGCC
3'	CCTCGCCCCGGACCTGCCCTCCCGCCAGGTGCACCC ACCTGC**AATAAA**TGCAGCGAAGCCGGGA

Table S2 shows the sequence of the human CYBA gene UTRs from the 5' to the 3' end. The polyadenylation signal (PAS) of the 3' UTR is shown in bold letters and the insulin 3'UTR stability element (INS_SCE) is underlined. The 5' UTR consists of 36 base pairs, whereas the 3' UTR contains 64 base pairs. Noteworthy, both UTRs are shorter than average human UTRs, for instance 5' UTRs consist of around 200 nucleotides and in case of 3'UTRs the average length is approximately 1000 nucleotides.

Transfection efficiencies on microstructured substrates

The percentage of successfully transfected cells was assessed to compare two different transfection agents and to ensure that transfection efficiencies were not hampered by microstructured cell growth (see Figure S1). Here, all cells grew on microstructured protein arrays. We obtained higher transfection efficiencies for Lipofectamine^{TM}2000 as compared to DOGTOR. Using a commercial Live/Dead cell viability assay (Molecular Probes, Germany), we found high cell viability rates above 80% (data not shown).

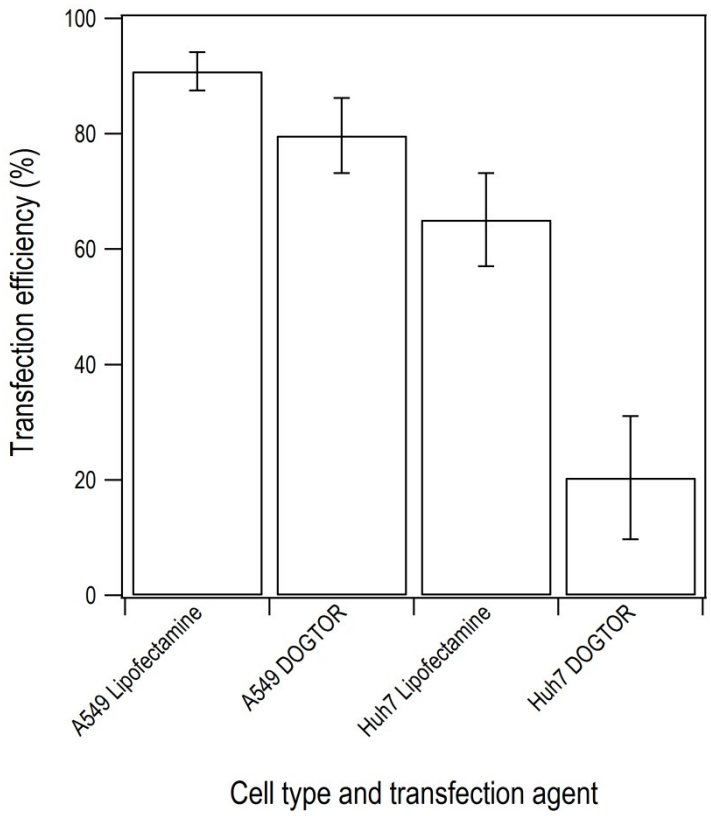

Figure S1. Transfection efficiencies on microstructured substrates. Percentage of transfected cells and corresponding standard deviations for A549 cells and Huh7 cells transfected with SNIM RNA with help of Lipofectamine™2000 or DOGTOR. We find higher transfection efficiencies for cells transfected with Lipofectamine™2000.

Area under the curve (AUC)

Assuming biochemical rate equations (4) and (5) for translation and degradation according to Fig. 3C, the amount of expressed protein after mRNA transfection is given by

$$G_{d2EGFP}(t) = \frac{K}{\delta - \beta} \cdot \left(1 - e^{-(\delta-\beta)(t-t_0)}\right) e^{-\beta(t-t_0)} \qquad \text{(Equation 1 of the main text).}$$

The area under the curve (AUC) is calculated by integrating the expression level $G_{d2EGFP}(t)$ from t_0, when expression sets in to long times ($t \to \infty$):

$$AUC = \int_{t=t_0}^{t=\infty} G(t) = \frac{K}{\delta - \beta} \int_0^{\infty} \left[e^{-\beta\tau} - e^{-\delta\tau}\right] d\tau = \frac{K}{\delta - \beta} \cdot \left[\frac{1}{\beta} - \frac{1}{\delta}\right] = \frac{K}{\delta \cdot \beta}$$

with $\tau = t - t_0$.

Using $\tau_{mRNA} = ln2/\delta$, $\tau_{d2EGFP} = ln2/\beta$, and $K = m_0 \cdot k_{TL}$ we obtain equation 3 of the main text:

$$AUC = 0.48 \cdot m_0 \cdot k_{TL} \cdot \tau_{mRNA} \cdot \tau_{d2EGFP}$$

The time course of $G_{d2EGFP}(t)$ and the AUC is schematically depicted in Figure 6A.

The experimental single-cell AUC distributions can be seen in Figure S2. Because the AUC depends linearly from the mRNA and protein life times, the single-cell AUC distributions are closely related to the mRNA and protein half-life distributions that are shown in Figure 4B and 4C of the main text.

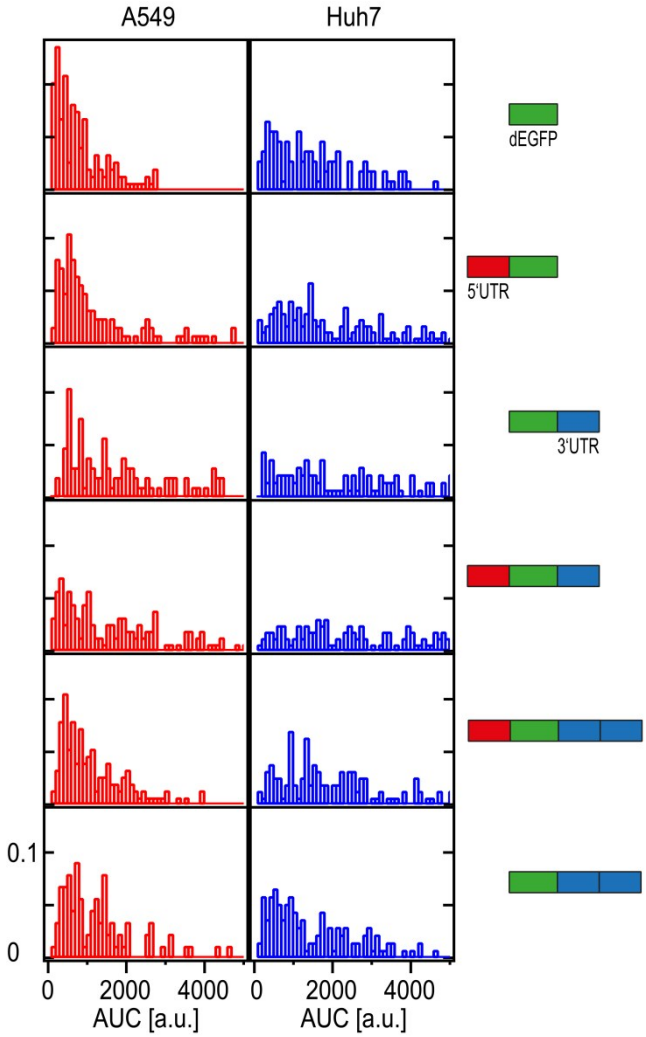

Figure S2. Distribution of the single-cell AUCs. AUCs were calculated according to equation 3 of the main text. A549 data are shown in red, Huh7 data are shown in blue.

Degradation rate of the reporter protein

To check the fitted d2EGFP degradation rates, we independently measured the degradation rate of d2EGFP inside A549 and Huh7 cells in microstructured six-channel slides. Protein synthesis was blocked by the antibiotic cycloheximide, which interferes with peptidyl transferase activity (3). Single-cell fluorescence intensity time courses were monitored for approximately 20h (see Figure S3). Control experiments ensured that the decrease in fluorescence intensity was not due to photobleaching of the chromophore. Single-cell time courses were fitted by a single exponential fit, yielding distributions of protein degradation rates. The mean degradation rates were found to be 0.28/h (std 0.08/h) in A549 cells and 0.17/h (std 0.08/h) in Huh 7 cells, corresponding to protein life times of 2.46 h and 4.04 h, respectively. Although these life times are significantly shorter than the life times as determined by single-cell time course analysis of mRNA mediated protein expression, the ratio between the mean life times of d2EGFP inside Huh7 and A549 cells is the same (4.04 h/2.46 h=1.64 as measured by translational blocking compared to 7.4 h/4.5 h=1.64 as determined by fitting the analytical solution for mRNA expression).

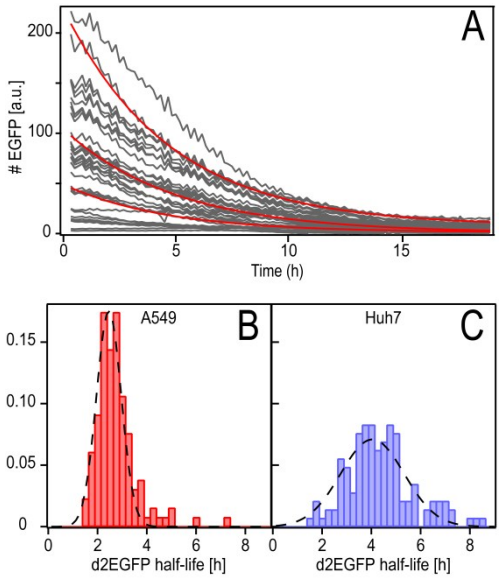

Figure S3. Distributions of directly measured d2EGFP half-lives. **(A)** Exemplary time courses of cycloheximide-induced d2EGFP degradation in Huh7 cells. Red lines are simple exponential fits for protein degradation. **(B)** Distribution of d2EGFP half-lives measured in A549 cells, yielding a mean half-life of 2.46 h (std 0.71 h). **(C)** Distribution of d2EGFP half-lives measured in Huh7 cells, yielding a mean half-life of 4.04 h (std 1.82 h).

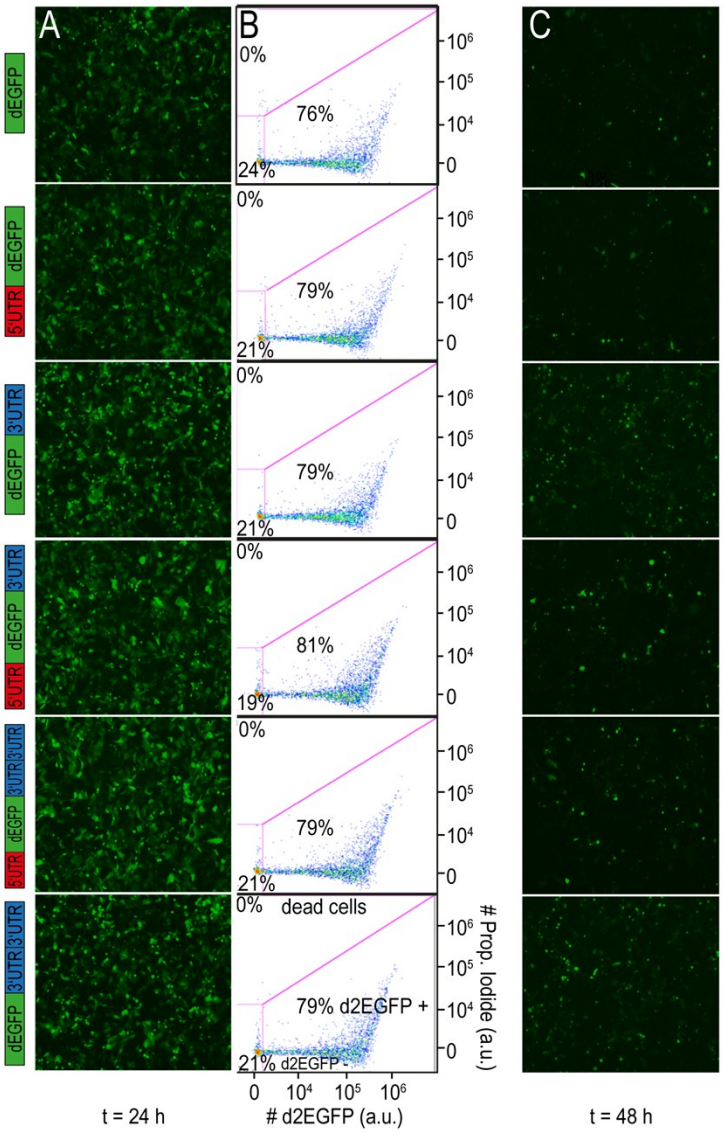

Figure S4. Fluorescence microscopy and flow cytometry data of Huh7 cells. **(A)** Fluorescence microscopy pictures taken with 4x magnification (JULY^{TM}) at 24 h post-transfection. All constructs showed improved protein expression levels as compared to the control. **(B)** The percentage of d2EGFP positive cells as determined by FC is similar for all constructs. Propidium iodide was used to detect dead cells. The applied gates ensured exclusion of dead cells and untransfected cells. **(C)** At 48 h post transfection, sustained protein expression was higher for the stabilized constructs as compared to the control.

Determination of physical mRNA half-life by qRT-PCR in A549 and Huh7 cells

In an additional experiment, we investigated the physical mRNA half-life of the different mRNA constructs with qRT-PCR, which is a conventional approach (see Figure S5). Therefore, the mRNA constructs were transfected as described in Materials & Methods. At the end, we obtained the absolute mRNA amount at each specific time point and calculated the physical mRNA half-life for each mRNA furnished with UTRs. We could detect an

increase of mRNA stability for mRNA furnished with 5'+3' UTR. However, no significant physical mRNA stabilization effects for any of the selected mRNA constructs as compared to the control were observed.

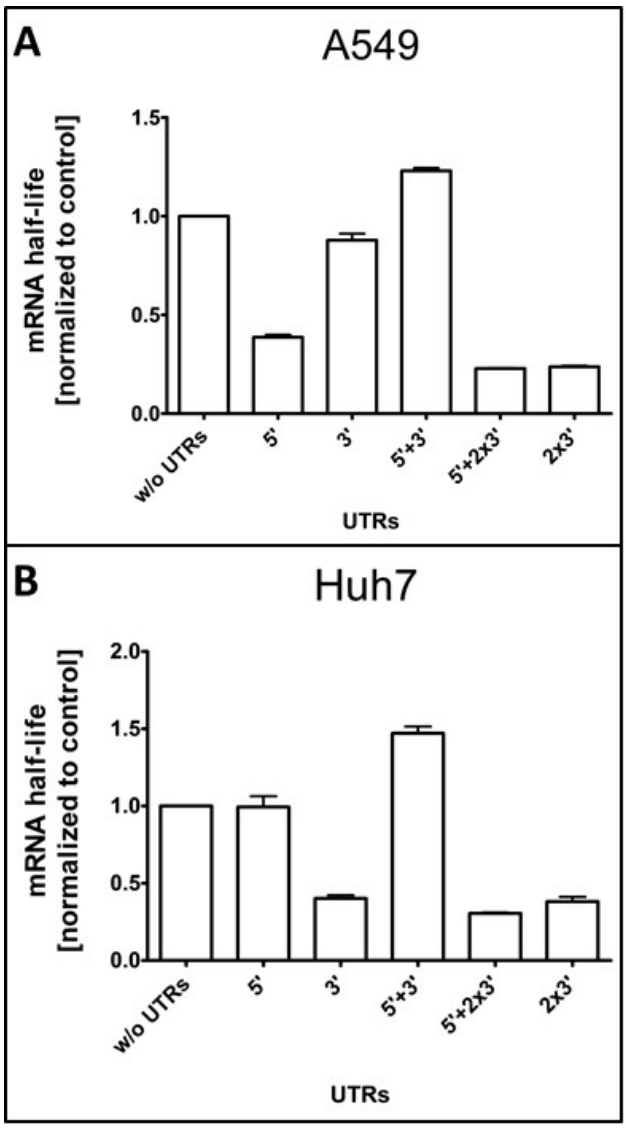

Figure S5 **Determination of physical mRNA half-life by qRT-PCR in A549 and Huh7 cells**

The cells were transfected according to the protocol in Materials & Methods part. Absolute mRNA quantification at 4, 8, 24, 36, 48, 60, 72 hours for all mRNA constructs was determined in A549 (see Figure S5 A) and in Huh7 (see Figure S5 B). Out of this data the physical mRNA half-life was calculated. The physical half-lives were normalized to the control.

Supplementary References

1. Zuker, M. (2003) Mfold web server for nucleic acid folding and hybridization prediction. *Nucleic acids research*, **31**, 3406-3415.
2. Babendure, J.R., Babendure, J.L., Ding, J.-H. and Tsien, R.Y. (2006) Control of mammalian translation by mRNA structure near caps. *RNA (New York, N.Y*, **12**, 851-861.
3. Siegel, M.R. and Sisler, H.D. (1963) Inhibition of Protein Synthesis in vitro by Cycloheximide. *Nature*, **200**, 675-676.